

# Identification and validation of a three-gene signature as a candidate prognostic biomarker for lower grade glioma

Kai Xiao<sup>1</sup>, Qing Liu<sup>1</sup>, Gang Peng<sup>1</sup>, Jun Su<sup>1</sup>, Chao-Ying Qin<sup>1</sup>, Xiang-Yu Wang<sup>Corresp. 1</sup>

<sup>1</sup> Department of Neurosurgery, Xiangya hospital of Central South University, Xiangya hospital, changsha, hunan, CHN

Corresponding Author: Xiang-Yu Wang  
Email address: wxyMGH@gmail.com

**Background** Lower grade glioma (LGG) are a heterogeneous tumor that may develop into high-grade malignant glioma seriously shortens patient survival time. The clinical prognostic biomarker of lower-grade glioma is still lacking. The aim of our study is to explore novel biomarkers for LGG that contribute to distinguish potential malignancy in low-grade glioma, to guide clinical adoption of more rational and effective treatments.

**Methods** The RNA-seq data for LGG was downloaded from the UCSC Xena and Chinese Glioma Genome Atlas (CGGA). By robust likelihood-based survival model, LASSO regression and multivariate Cox regression analysis, we developed a three-gene signature and established a risk score to predict the prognosis of patient with LGG. The three-gene signature was an independent survival predictor compared to other clinical parameters. Based on the signature related risk score system, stratified survival analysis was performed in patients with different age group, gender, and pathologic grade. The prognostic signature was validated in CGGA dataset. Finally, Weighted Gene Co-expression Network Analysis (WGCNA) was carried out to find the co-expression genes related to the member of the signature and enrichment analysis of Gene Ontology (GO) and Kyoto Encyclopedia of Genes and Genomes (KEGG) pathway were conducted for those co-expression network. To prove the superiority of the model, time-dependent ROC curves of our model and other models are constructed. **Results** In this study, a three-gene signature (WEE1, CRTAC1, SEMA4G) was constructed. Based on the model, the risk score of each patient was calculated with LGG (low-risk vs. high-risk, hazard ratio[HR]=0.198, 95%CI=0.120-0.325) and patients in the high-risk group had significantly poorer survival results than those in the low-risk group. Furthermore, the model was validated in CGGA dataset. Lastly, by WGCNA, we constructed the co-expression network of the three genes and conducted the enrichment of GO and KEGG. Our study identified a three-gene model that showed better performance in predicting the 1-, 3- and 5-year survival of LGG patients compared to other models and may be promising independent biomarker of LGG.

1 **Identification and validation of a three-gene signature as a candidate prognostic biomarker**  
2 **for lower grade glioma**

3 **Kai Xiao<sup>1</sup>, Qing Liu<sup>1</sup>, Gang Peng<sup>1</sup>, Jun Su<sup>1</sup>, Chao-Ying Qin<sup>1</sup>, Xiang-Yu Wang<sup>1</sup>**

4 1. Department of Neurosurgery, Xiangya hospital of Central South University, Changsha  
5 410008, Hunan Province, People's Republic of China

6 Corresponding Author:

7 Xiang-Yu Wang, [wxyMGH@gmail.com](mailto:wxyMGH@gmail.com)

8 Xiangya road, kaifu district, Changsha, Hunan province, 410008, People's Republic of China

9 **Abstract**

10 **Background**

11 Lower grade glioma(LGG) are a heterogeneous tumor that may develop into high-grade  
12 malignant glioma seriously shortens patient survival time. The clinical prognostic biomarker of  
13 lower-grade glioma is still lacking. The aim of our study is to explore novel biomarkers for LGG  
14 that contribute to distinguish potential malignancy in low-grade glioma, to guide clinical  
15 adoption of more rational and effective treatments.

16 **Methods**

17 The RNA-seq data for LGG was downloaded from the UCSC Xena and Chinese Glioma  
18 Genome Atlas (CGGA). By robust likelihood-based survival model, LASSO regression and  
19 multivariate Cox regression analysis, we developed a three-gene signature and established a risk  
20 score to predict the prognosis of patient with LGG. The three-gene signature was an independent  
21 survival predictor compared to other clinical parameters. Based on the signature related risk  
22 score system, stratified survival analysis was performed in patients with different age group,  
23 gender, and pathologic grade. The prognostic signature was validated in CGGA dataset.  
24 Finally, Weighted Gene Co-expression Network Analysis (WGCNA) was carried out to find the  
25 co-expression genes related to the member of the signature and enrichment analysis of Gene  
26 Ontology(GO) and Kyoto Encyclopedia of Genes and Genomes(KEGG) pathway were  
27 conducted for those co-expression network. To prove the superiority of the model, time-

28 dependent ROC curves of our model and other models are constructed.

## 29 **Results**

30 In this study, a three-gene signature(WEE1, CRTAC1, SEMA4G)was constructed. Based on  
31 the model, the risk score of each patient was calculated with LGG(low-risk vs. high- risk,  
32 hazard ratio[HR]=0.198, 95%CI= 0.120-0.325) and patients in the high-risk group had  
33 significantly poorer survival results than those in the low-risk group. Furthermore, the model  
34 was validated in CGGA dataset. Lastly, by WGCNA, we constructed the co-expression network  
35 of the three genes and conducted the enrichment of GO and KEGG. Our study identified a three-  
36 gene model that showed better performance in predicting the 1-, 3- and 5-year survival of LGG  
37 patients compared to other models and may be promising independent biomarker of LGG.

38 **Keyword:** low-grade glioma, prognosis, WGCNA, risk score, robust likelihood-based survival  
39 model, biomarker, signature, better performance

## 40 **Introduction**

41 With the development of sequencing and bioinformatics technologies, accumulating studies  
42 have revealed that different patients may be similar in glioma grade but differ greatly in  
43 molecular characteristics, clinical prognosis, and treatment response. So many central nervous  
44 system tumors were named according to molecular parameters and histopathologic diagnosis,  
45 especially gliomas, ependymomas, and medulloblastomas in the 2016 revision of the WHO  
46 classification(Zhang et al. 2019b). As we know, some molecular markers, such as MGMT(O6-  
47 methylguanine DNA methyltransferase)(Binabaj et al. 2018), IDH(isocitrate dehydrogenase)  
48 (Kwon et al. 2019), EGFR(epidermal growth factor receptor)(Chistiakov et al. 2017), and  
49 PTEN(phosphatase and tensin homolog)(Koshiyama et al. 2017)that have contributed to  
50 personalized therapeutic approaches and targeted anti-glioblastoma therapies have been routinely  
51 tested in glioblastoma patients clinically. However there are few specific clinical indicators and  
52 therapeutic targets for LGGs compared to glioblastoma, so it is urgent to elucidate the  
53 mechanism of glioma development and progression, which can provide potential treatment  
54 targets for LGGs.

55 In this study, gene expression RNAseq data and corresponding clinical information of LGG

56 patients were downloaded from UCSC Xena(<https://xenabrowser.net/hub/>) and Chinese Glioma  
57 Genome Atlas (CGGA,<http://www.cgga.org.cn/>). By analyzing data from UCSC Xena using  
58 robust likelihood-based survival model and Cox regression, we developed a three-gene signature  
59 that provides effective survival risk stratification of patients with LGG and validated the  
60 signature in the CGGA dataset. These results demonstrate the potential of the three-gene  
61 signature for survival prediction of patients with LGG and provide new potential molecular  
62 treatment targets for LGGs.

## 63 **Materials and Methods**

### 64 **Dataset of Patients with LGG**

65 The LGGs RNA sequencing (RNAseq) data and corresponding clinical information were  
66 downloaded from The Cancer Genome Atlas (TCGA) hub by the University of California, Santa  
67 Cruz, Xena browser(<https://xenabrowser.net/hub/>) and CGGA data  
68 portal(<http://www.cgga.org.cn/>) respectively. The TCGA RNAseq data (level 3) shows the gene-  
69 level transcription estimates, as in  $\log_2(x+1)$  transformed RSEM normalized count. The CGGA  
70 data displays the gene expression level as fragments per kilobase transcriptome per million  
71 fragments(FPKM), which has been standardized. Expressed gene defined only if its expressed  
72 level is larger than 0 at half of samples. Only patients with a clear information of survival and  
73 detailed history of radiotherapy and chemotherapy/molecular therapy were included in the study.  
74 Finally, 456 cases from TCGA dataset and 159 cases from the CGGA dataset were included in  
75 the training set and validation set respectively. **Table 1** summarized the clinical characteristics  
76 and therapy information of the training set and validation set. The workflow presentation of this  
77 study is shown in **Figure 1**.

### 78 **Identification of survival-related genes and construction of the prognostic model**

79 By using the rbsurv package in R, a robust likelihood-based survival model was conducted to  
80 identify survival-related genes(Cho et al. 2009). The rbsurv package is a software program, which  
81 selects survival-associated genes based on the partial likelihood of the Cox model and adopts a  
82 cross-validation approach for robustness. According to the description of the rbsurv package, prior

83 gene selection such as univariate survival modeling can be performed if necessary and the  
84 univariate survival modeling can be performed in this software program. Compared to the survival  
85 modeling without an adjustment of risk factors, the robust likelihood-based survival model can  
86 improve the ability to discover truly survival-associated genes by modeling genes after adjusting  
87 for certain risk factor. Thus, we directly conduct a robust likelihood-based survival model to  
88 screen for the prognostic genes. The robustness test was performed on 20530 genes and 456  
89 samples. After 10 iterations, 29 prognostic related genes were selected. With the help of glmnet  
90 and survival package in R, least absolute shrinkage and selection operator (LASSO) regression and  
91 the multivariable Cox proportional hazard regression method were used to further identify the  
92 survival-related prognostic model. The same approach was used to identify gene signatures for  
93 endometrial carcinoma (Ouyang et al. 2019). At last, three prognostic survival-related genes that  
94 were independent survival predictors and their regression coefficients were obtained at a threshold  
95 of  $P < 0.05$ . Based on the median expression value of each survival-related gene, we dichotomized  
96 456 LGGs patients into low and high expression groups and compare the survival rate between the  
97 two groups by Kaplan-Meier plots and Log-rank test. According to the estimated regression  
98 coefficients, a prognostic risk score for each patients was then calculated (Wang et al. 2019). The  
99 risk score =  $(0.4470 \times \text{expression level of WEE1}) + (-0.1530 \times \text{expression level of CRTAC1}) + (-$   
100  $0.3723 \times \text{expression level of SEMA4G})$ . With the three-gene signature, 456 LGGs patients were  
101 divided into high-risk and low-risk groups with the median risk score as the cut-off value. Kaplan-  
102 Meier curves were performed to estimate and compare the survival for TCGA LGGs patients with  
103 a high score or a low score. The receiver operating characteristic (ROC) curve and area under the  
104 curve (AUC) were applied to evaluate the prediction accuracy of the risk score model. Furthermore  
105 stratified survival analysis was performed in patients with different age group (younger, old),  
106 gender (male, female), and pathologic grade (G2, G3).  
107 Univariate and multivariate Cox hazard regression analysis were conducted for the potential  
108 prognostic factors such as age group (younger vs. old), gender (male vs. female), pathologic

109 grade(G2 vs. G3), radiation therapy(Yes vs. No), molecular therapy(Yes vs. No) and risk  
110 score(High vs. Low).

### 111 **Validation of the prognostic model in the CGGA**

112 The prognostic model was validated in the CGGA mRNAseq\_325 cohort. Only patients with a  
113 clear information of survival, detailed history of radiotherapy and chemotherapy were included  
114 in the study. Finally, 159 cases from the CGGA mRNAseq\_325 cohort were included in the  
115 validation set.

### 116 **Exploring co-expression genes by WGCNA**

117 To explore the regulatory network of the three genes, WGCNA was performed in training set by  
118 the R package WGCNA(Langfelder & Horvath 2008). The top 50% variance of genes were  
119 selected for WGCNA. In other words, WGCNA based on 456 samples and 10256 genes. First,  
120 RNAseq data were filtered to reduce outliers. Using the absolute value of the correlation between  
121 the expression levels of transcripts, a co-expression similarity matrix was constructed. Then, the  
122 co-expression similarity matrix was transformed to the adjacency matrix by choosing 9 as a soft  
123 threshold. Co-expression gene module was established by the topological overlap measure. In  
124 order to identify the significance of each module, gene significance(GS) was calculated to  
125 estimate the correlation between genes and sample traits. Module significance(MS) was defined  
126 as the average GS within modules and was calculated to measure the correlation between  
127 modules and sample traits(vital status). Finally, the “vital status” related modules that contain  
128 the 3 genes as members and genes belong to such modules were identified. Genes interacted with  
129 those three genes were screened and the co-expression network was constructed by Cytoscape  
130 software(Shannon et al. 2003).

### 131 **Functional enrichment analysis**

132 Using Enrichment analysis of Gene Ontology(GO) and Kyoto Encyclopedia of Genes and  
133 Genomes(KEGG) pathway were conducted via the clusterProfiler package in R language(Yu et  
134 al. 2012) for those genes that belong to the “vital status” related modules associated with the  
135 three genes. Benjamini-Hochberg (BH)-adjusted p-value <0.05 were considered significant.

## 136 Results

### 137 Three prognostic genes were identified in TCGA dataset and validated in CGGA dataset

138 456 patients and 20530 genes were included in the TCGA-LGG to train the prognostic model.

139 The robust likelihood-based survival model found 29 survival-related genes, 13 genes were  
140 obtained through LASSO Cox method(Fig.2). We further reduced the dimensionality of these  
141 high-dimensional data by multivariate Cox proportional hazard regression model. Finally, three  
142 genes that were independent survival predictors were identified as survival prediction signature.

143 Those three genes included in the model were WEE1, SEMA4G, CRTAC1. It has been reported  
144 that WEE1 is closely related to the growth, invasion and migration of glioma(Wu et al. 2019).

145 Currently, there is no study revealing the role of SEMA4G and CRTAC1 in gliomas. After

146 calculating the risk score, patients were divided into a high- and low-risk group based on the

147 median cut-off point of the risk score. The three-gene signature risk score distribution is shown

148 in Fig 3A. Besides, the relationship between risk score and the status of the LGGs was

149 calculated(Fig.3B). As shown in the heat map of the Figure 3C, a remarkable high expression

150 was noted for WEE1 in the high-risk group, while a lower expression was observed for the other

151 genes in the high-risk group.(Fig.3C). Patients in the high-risk group were significantly worse off

152 the overall survival time compared to the low-risk group( $P < 0.0001$ )(Fig.4A). The area under

153 ROC curve of the signature for 1-,3- and 5-year overall survival was 0.904,0.878 and 0.805,

154 respectively, in training set. (Fig.4B). A similar result can be noted in the validation

155 dataset(Fig.4C). The area under ROC curve of the signature for 1-,3- and 5-year overall survival

156 was 0.783,0.813 and 0.813, respectively, in validation set. (Fig.4D).Moreover, the predicting

157 power of the risk score model was not decreased in subgroup analysis for age

158 group(younger, $P=0.00012$ ;old, $P < 0.0001$ ) , gender(male, $P < 0.0001$ ;female, $P < 0.0001$ ), and

159 pathologic grade(G2, $P=0.00013$ ;G3, $P < 0.0001$ ) in the training set(Fig.5A-5F). The same trend

160 can be observed in the validation dataset(Fig.6A-6F).For the WEE1, the member of high

161 expression group had significantly shorter survival than those in low expression group( $P <$

162  $0.0001$ )(Fig.7A). For the SEMA4G and CRTAC1, the member of high expression group had

163 significantly longer survival than those in low expression group( $P < 0.0001$ )([Fig.7B-7C](#)). The  
164 expression level of WEE1 was significantly higher in grade III compared to grade II( $P <$   
165  $0.0001$ ), while the other are opposite([Fig.8A](#)). These results can also be verified in the validation  
166 dataset([Fig.7D-7F, 8B](#)).

167 Multivariate Cox proportional hazard regression demonstrated that age group (HR=0.274, P=  
168  $2.21E-09$ ), pathologic grade (HR=2.49, P=0.00011) and risk score(HR=0.198, P <  
169  $0.000000000168$ ) were independent prognostic factors in the training set, while pathologic  
170 grade(HR=3.799, P=0.00000151), 1p19q status(HR=4.566, P=0.0000388), radiation therapy  
171 (HR=0.524, P=0.046), and risk score (HR=0.415, P=0.000653)were independent prognostic  
172 factors in validation dataset([Table 2](#)) .

### 173 **Calculation of module-trait correlation in LGGs and module visualization of the network** 174 **connections**

175 Using the R package WGCNA, gene modules were identified based on the top 50% variance of  
176 genes. To analyze the relationship between gene modules and sample clinical information, we  
177 used the module eigengene(ME) as the overall gene expression level of the corresponding  
178 modules and calculated correlations with clinical phenotypes, for example, vital status. we  
179 obtained 16 gene modules ([SupplementFigure1.A-D](#)) with size ranging from 31 to 1501 genes.  
180 We assigned each co-expression module an arbitrary color for reference: black, blue, brown,  
181 cyan, green, greenyellow, lightcyan, magenta, midnightblue, pink, purple, red, salmon, tan,  
182 turquoise, and yellow. These modules contained 449, 1352, 850, 46, 519, 91, 31, 201, 43, 336,  
183 135, 462, 51, 90, 1501 and 845 genes, respectively. As a single group, the non-co-expressed  
184 group designated as 'grey' based on the WGCNA developer's rationale. Vital status related  
185 modules, such as yellow, green, black modules that contain the 3 genes as members and genes  
186 belong to such modules were screened([SupplementFigure1.D](#)). Finally, 32 genes were  
187 discovered to be co-expressed with CRTAC1, 181 genes were co-expressed with WEE1, 6  
188 genes with SEMA4G. We exported the screened genes and three prognostic survival-related  
189 genes into Cytoscape and constructed the co-expression network([Fig.9](#)).

## 190 **GO and KEGG analysis of screened genes interacted with three-gene signature**

191 For the “biological processes”(BP), chromosome segregation, nuclear division, mitotic nuclear  
192 division, organelle fission, mitotic sister chromatid segregation were the commonly enriched  
193 categories(Fig.10A). For the “cellular component”(CC), the enriched categories were correlated  
194 with condensed chromosome, chromosome/centromeric region, chromosomal region,  
195 kinetochore, condensed chromosome/centromeric region(Fig.10B). For the “molecular function”  
196 (MF), these screened genes mainly enriched in microtubule binding, tubulin binding, histone  
197 kinase activity, DNA-dependent ATPase activity, protein serine/threonine kinase  
198 activity(Fig.10D).KEGG pathway enrichment analysis suggested that cell cycle was the most  
199 important pathway for these selected genes. The following pathway also involved many screened  
200 genes, including, oocyte meiosis, progesterone-mediated oocyte maturation, fanconi anemia  
201 pathway, homologous recombination(Fig.10C).Additionally, For the Gene Ontology analysis,  
202 these 3 co-expression gene modules (yellow, green, black) enriched results can be seen in  
203 supplemental files(SupplementalFigure2, 3).

## 204 **A comparison between our and other models**

205 Recently, Chen X.P et al reported a model containing 3 genes(EMP3、GSX2、EMILIN3) based  
206 on integrative analysis of DNA methylation and gene expression in TCGA dataset(Zeng et al.  
207 2018).Chuang Zhang et al also reported a 4-gene(EMP3、GNG12、KIF2C、IFI44) prognostic  
208 signature based on genes encodes by chr1p/19q(Zhang et al. 2019a). To compared the prognostic  
209 values of our prognostic signature and their model, we performed time-dependent ROC curve  
210 analysis in our model and other models based on the risk score calculated by the regression  
211 coefficients which obtained by themselves and the expression level of members in their signature  
212 showed in the TCGA dataset, which has a larger number of samples compared to CGGA dataset,  
213 that might be able to ensure the credibility of the comparison results. The results exhibited that  
214 our model displayed a better predictive value in predicting 1-, 3- and 5-year overall survival  
215 compared to other models, especially in 1-, 3-year overall survival(Fig.11A-11C). In other  
216 words, our 3-gene model had a better efficiency in predicting both short- and long-term

217 prognosis.

## 218 **Discussion**

219 From the perspective of traditional pathology, the diagnosis of low-grade glioma depends on  
220 pathological type and pathological grade. With the development of sequencing technology,  
221 molecular biomarkers for the diagnosis of LGG have attracted widespread attention(Cancer  
222 Genome Atlas Research et al. 2015). Prognostic factors for the low-grade glioma that are well  
223 known include IDH mutations(Batsios et al. 2019), 1p/19q co-deficiency(Zhang et al. 2019a),  
224 ATRX mutation(Ren et al. 2019), TERT promoter mutations(Chan et al. 2015), CIC loss(Sahm  
225 et al. 2012), FUBP1 loss(Sahm et al. 2012) and PTEN loss(Sabha et al. 2014) and the above  
226 prognostic marker contribute to clinicians to understand the mechanism of low-grade gliomas.  
227 The complex pathogenesis of LGG encourages us to explore more prognostic markers for further  
228 understand it and develop an efficient treatment.

229 In this study, we identified three genes that were closely correlated with LGG prognosis.  
230 Considering the differentially expressed genes(DEGs) between tumor and normal tissue might  
231 not be associated with survival(Liu et al. 2019) and the univariate survival modeling can be  
232 performed in rbsurv package, the robust likelihood-based survival model was performed using  
233 the rbsurv package in R as the first step instead of screening for DEGs and conducting the  
234 univariate Cox regression. LASSO and Cox proportional hazard regression model are widely  
235 used to generate prognostic genes in the context of high dimensional data, thus were adopted in  
236 subsequent analysis. Compared to a single predictive biomarker, integrating multiple biomarkers  
237 into a signature is believed to be more predictive. The risk score calculated by the risk model was  
238 considered to have good predictive capabilities and was demonstrated to be an independent  
239 prognostic factor after adjusting the effects of age, sex, tumor grade, molecular therapy and  
240 radiation therapy. The risk score was confirmed to be effective in different age groups, gender  
241 and pathologic grade. Regardless of the training set or the validation set, the AUC value of 1-,  
242 3- and 5-year was greater than 0.75. The pathologic grade and the risk level were confirmed to  
243 be independent prognostic factors both in training set and validation set.

244 In order to construct a co-expression network of the three genes, WGCNA was used in the  
245 training set. We found the survival related modules to which these three genes belong, and  
246 extracted the genes of these three modules to construct a co-expression network. Finally, 32  
247 genes were discovered to be co-expressed with CRTAC1, 181 genes were co-expressed with  
248 WEE1, 6 genes with SEMA4G. The co-expression network of the three genes is visualized by  
249 Cytoscape in Figure 9.

250 Based on the result of GO and KEGG enrichment analysis of these co-expression genes,  
251 “condensed chromosome” was the most significant enrichment in CC. Coincidentally, Rebecca  
252 C et al. found that interference with chromatin condensation results in failure to fully activate  
253 DNA damage response(Burgess et al. 2014) and the DNA damage response triggers multiple  
254 cellular events including activation of DNA repair pathway, arrest of the cell cycle to allow time  
255 for repair, and, in certain cases, initiation of senescence or apoptosis programs(Ciccia &  
256 Elledge 2010). For the BP category, chromosome segregation was the most enrichment and  
257 research has proven that chromosome instability contributes to the development of genetic  
258 heterogeneity in tumors and allows the outgrowth of tumorigenic cells with advantageous  
259 karyotypes(Conde et al. 2017). Regarding the MF category, microtubule binding was the most  
260 influential and the drug targeted microtubule was proven effective in glioma. For example, the  
261 drug EM011 functions by disrupting microtubule dynamics and modules several oncogenic  
262 mediators causing a decrease in cell viability, proliferation and migration/invasion in the  
263 astrocytoma cell lines(Ajeawung et al. 2013). For KEGG pathway enrichment analysis, cell  
264 cycle was the most significant pathway. Stephen D has explained that signaling pathway  
265 converge on the cell cycle machinery to regulate developmental genes and execute cell fate  
266 decisions(Dalton 2015).

267 The three-gene signature provided a wealth of potential biological and therapeutic information  
268 about LGG.WEE1(WEE1 G2 checkpoint kinase), located on the short arm of human  
269 chromosome 11(11p15.4), encodes a nuclear protein, which is a tyrosine kinase belonging to the  
270 Ser/Thr family of protein kinases. The protein catalyzes the inhibitory tyrosine phosphorylation

271 of CDC2/cyclin B kinase, and appears to coordinate the transition between DNA replication and  
272 mitosis by protecting the nucleus from cytoplasmically activated CDC2 kinase. WEE1 has been  
273 confirmed that its protein expression increases with malignancy grade(Music et al. 2016).  
274 Moreover, patients with high WEE1 expression had poor survival than did patients with low  
275 WEE1 expression in grade III gliomas(Music et al. 2016).CRTAC1, cartilage acidic protein 1, a  
276 novel human marker which allowed discrimination of human chondrocytes from osteoblasts and  
277 mesenchymal stem cells in culture can be divided into CRTAC1-A and CRTAC1-B two  
278 subtypes according to the last exon. Previous study found that inhibition of CRTAC1 reduces  
279 ultraviolet B irradiation induced-apoptosis through P38 mitogen-activated protein kinase and jun  
280 Amino-Terminal kinase pathway(Ji et al. 2016). It means that the relationship between the  
281 expression of CRTAC1 and apoptosis is positively correlated after ultraviolet B irradiation. To  
282 some extent, this is consistent with our finding that CRTAC1 high expression prolongs survival  
283 time in LGG patients. However, its detailed mechanism in LGG remains to be further explored.  
284 Semaphorins are a large family of conserved secreted and membrane associated proteins which  
285 possess a semaphoring(Sema) domain and a PSI domain in the N-terminal extracellular portion.  
286 Based on sequence and structural similarities, semaphorins are put into eight classes:  
287 invertebrates contain classes 1 and 2, viruses have class 8, and vertebrates contain class 3-7.  
288 Semaphorins serves as axon guidance ligands via multimeric receptor complexes, some  
289 containing plexin proteins. Semaphorins and Plexins are cognate ligand-receptor families that  
290 regulate important steps during nervous system development(Maier et al. 2011). A low-  
291 expression of SEMA4G was detected in colorectal cancer tissues compared with normal tissues.  
292 It means that SEMA4G might be a tumor suppressor gene related to colorectal cancer(Wang et  
293 al. 2008). However, little work has been done to elucidate the role of SEMA4G in glioma. Our  
294 study demonstrated that SEMA4G was significantly down-regulated in grade III patients  
295 compared to grade II and the high-expression of SEMA4G was associated with a good prognosis  
296 in LGG patients. Further work is needed to explore its functions in LGG. To sum up, the three-  
297 gene signature could predict LGG survival based on a risk score model. We firmly believed that

298 these genes are potential prognostic markers or therapeutic targets for LGG patients.

299 Nevertheless, the molecular mechanisms how the three-gene signature affected the prognosis of  
300 LGG patients should be further elucidated by a series of experiments.

### 301 **Conclusion**

302 In conclusion, Our study identified a 3-gene model that showed better performance in predicting  
303 short- and long-term survival of LGG patients compared to other models. Moreover, our finding  
304 provided new insights into the pathogenesis and prognosis of LGG.

### 305 **Acknowledgments**

306 We thank editors for constructive comments on a previous version of this manuscript.

### 307 **Additional information and declarations**

### 308 **Funding statement**

309 This work was funded by grants from the National Nature Science Foundation of China(NO 81801908)and the  
310 National Key Technology Research and Development Program of the Ministry of Science and Technology of  
311 China(NO 2014BAI04B01, NO 2014BAI04B02 and NO 2015BAI12B04). There was no additional external  
312 funding received for this study.

### 313 **Competing Interests**

314 The authors report no conflicts of interest in this work.

### 315 **Author Contributions**

316 All authors contributed to data analysis, drafting and revising the article, gave final approval of  
317 the version to be published, and agree to be accountable for all aspects of the work.

### 318 **Availability of data and material**

319 The following information was supplied regarding data availability:

320 All relevant data have been provided in the Supplemental Files.

### 321 **Supplemental Information**

322 Supplemental information for this article can be found at Supplemental Files.

### 323 **References**

324 Ajeawung NF, Joshi HC, and Kamnasaran D. 2013. The microtubule binding drug EM011 inhibits the growth of  
325 paediatric low grade gliomas. *Cancer Lett* 335:109-118. 10.1016/j.canlet.2013.02.004

326 Batsios G, Viswanath P, Subramani E, Najac C, Gillespie AM, Santos RD, Molloy AR, Pieper RO, and Ronen SM.

2019. PI3K/mTOR inhibition of IDH1 mutant glioma leads to reduced 2HG production that is associated with increased survival. *Sci Rep* 9:10521. 10.1038/s41598-019-47021-x

Binabaj MM, Bahrami A, ShahidSales S, Joodi M, Joudi Mashhad M, Hassanian SM, Anvari K, and Avan A. 2018. The prognostic value of MGMT promoter methylation in glioblastoma: A meta-analysis of clinical trials. *J Cell Physiol* 233:378-386. 10.1002/jcp.25896

Burgess RC, Burman B, Kruhlak MJ, and Misteli T. 2014. Activation of DNA damage response signaling by condensed chromatin. *Cell Rep* 9:1703-1717. 10.1016/j.celrep.2014.10.060

Cancer Genome Atlas Research N, Brat DJ, Verhaak RG, Aldape KD, Yung WK, Salama SR, Cooper LA, Rheinbay E, Miller CR, Vitucci M, Morozova O, Robertson AG, Noushmehr H, Laird PW, Cherniack AD, Akbani R, Huse JT, Ciriello G, Poisson LM, Barnholtz-Sloan JS, Berger MS, Brennan C, Colen RR, Colman H, Flanders AE, Giannini C, Grifford M, Iavarone A, Jain R, Joseph I, Kim J, Kasaian K, Mikkelsen T, Murray BA, O'Neill BP, Pachter L, Parsons DW, Sougnez C, Sulman EP, Vandenberg SR, Van Meir EG, von Deimling A, Zhang H, Crain D, Lau K, Mallery D, Morris S, Paulauskis J, Penny R, Shelton T, Sherman M, Yena P, Black A, Bowen J, Dicostanzo K, Gastier-Foster J, Leraas KM, Lichtenberg TM, Pierson CR, Ramirez NC, Taylor C, Weaver S, Wise L, Zmuda E, Davidsen T, Demchok JA, Eley G, Ferguson ML, Hutter CM, Mills Shaw KR, Ozenberger BA, Sheth M, Sofia HJ, Tarnuzzer R, Wang Z, Yang L, Zenklusen JC, Ayala B, Baboud J, Chudamani S, Jensen MA, Liu J, Pihl T, Raman R, Wan Y, Wu Y, Ally A, Auman JT, Balasundaram M, Balu S, Baylin SB, Beroukhi R, Bootwalla MS, Bowlby R, Bristow CA, Brooks D, Butterfield Y, Carlsen R, Carter S, Chin L, Chu A, Chuah E, Cibulskis K, Clarke A, Coetzee SG, Dhalla N, Fennell T, Fisher S, Gabriel S, Getz G, Gibbs R, Guin R, Hadjipanayis A, Hayes DN, Hinoue T, Hoadley K, Holt RA, Hoyle AP, Jefferys SR, Jones S, Jones CD, Kucherlapati R, Lai PH, Lander E, Lee S, Lichtenstein L, Ma Y, Maglinte DT, Mahadeshwar HS, Marra MA, Mayo M, Meng S, Meyerson ML, Mieczkowski PA, Moore RA, Mose LE, Mungall AJ, Pantazi A, Parfenov M, Park PJ, Parker JS, Perou CM, Protopopov A, Ren X, Roach J, Sabedot TS, Schein J, Schumacher SE, Seidman JG, Seth S, Shen H, Simons JV, Sipahimalani P, Soloway MG, Song X, Sun H, Tabak B, Tam A, Tan D, Tang J, Thiessen N, Triche T, Jr., Van Den Berg DJ, Veluvolu U, Waring S, Weisenberger DJ, Wilkerson MD, Wong T, Wu J, Xi L, Xu AW, Yang L, Zack TI, Zhang J, Aksoy BA, Arachchi H, Benz C, Bernard B, Carlin D, Cho J, DiCara D, Frazer S, Fuller GN, Gao J, Gehlenborg N, Haussler D, Heiman DI, Iype L, Jacobsen A, Ju Z, Katzman S, Kim H, Knijnenburg T, Kreisberg RB, Lawrence MS, Lee W, Leinonen K, Lin P, Ling S, Liu W, Liu Y, Liu Y, Lu Y, Mills G, Ng S, Noble MS, Paull E, Rao A, Reynolds S, Saksena G, Sanborn Z, Sander C, Schultz N, Senbabaoglu Y, Shen R, Shmulevich I, Sinha R, Stuart J, Sumer SO, Sun Y, Tasman N, Taylor BS, Voet D, Weinhold N, Weinstein JN, Yang D, Yoshihara K, Zheng S, Zhang W, Zou L, Abel T, Sadeghi S, Cohen ML, Eschbacher J, Hattab EM, Raghunathan A, Schniederjan MJ, Aziz D, Barnett G, Barrett W, Bigner DD, Boice L, Brewer C, Calatozzolo C, Campos B, Carlotti CG, Jr., Chan TA, Cuppini L, Curley E, Cuzzubbo S, Devine K, DiMeco F, Duell R, Elder JB, Fehrenbach A, Finocchiaro G, Friedman W, Fulop J, Gardner J, Hermes B, Herold-Mende C, Jungk C, Kendler A, Lehman NL, Lipp E, Liu O, Mandt R, McGraw M, McLendon R, McPherson C, Neder L, Nguyen P, Noss A, Nunziata R, Ostrom QT, Palmer C, Perin A, Pollo B, Potapov A, Potapova O, Rathmell WK, Rotin D, Scarpace L, Schilero C, Senecal K, Shimmel K, Shurkhay V, Sifri S, Singh R, Sloan AE, Smolenski K, Staugaitis SM, Steele R, Thorne L, Tirapelli DP, Unterberg A, Vallurupalli M, Wang Y, Warnick R, Williams F, Wolinsky Y, Bell S, Rosenberg M, Stewart C, Huang F, Grimsby JL, Radenbaugh AJ, and

- 368 Zhang J. 2015. Comprehensive, Integrative Genomic Analysis of Diffuse Lower-Grade Gliomas. *N Engl J*  
369 *Med* 372:2481-2498. 10.1056/NEJMoa1402121
- 370 Chan AK, Yao Y, Zhang Z, Chung NY, Liu JS, Li KK, Shi Z, Chan DT, Poon WS, Zhou L, and Ng HK. 2015.  
371 TERT promoter mutations contribute to subset prognostication of lower-grade gliomas. *Mod Pathol*  
372 28:177-186. 10.1038/modpathol.2014.94
- 373 Chistiakov DA, Chekhonin IV, and Chekhonin VP. 2017. The EGFR variant III mutant as a target for  
374 immunotherapy of glioblastoma multiforme. *Eur J Pharmacol* 810:70-82. 10.1016/j.ejphar.2017.05.064
- 375 Cho H, Yu A, Kim S, Kang J, and al e. 2009. Robust likelihood-based survival modeling with microarray data.  
376 *Journal of Statistical Software* 29.
- 377 Ciccia A, and Elledge SJ. 2010. The DNA damage response: making it safe to play with knives. *Mol Cell* 40:179-  
378 204. 10.1016/j.molcel.2010.09.019
- 379 Conde M, Michen S, Wiedemuth R, Klink B, Schrock E, Schackert G, and Temme A. 2017. Chromosomal  
380 instability induced by increased BIRC5/Survivin levels affects tumorigenicity of glioma cells. *BMC Cancer*  
381 17:889. 10.1186/s12885-017-3932-y
- 382 Dalton S. 2015. Linking the Cell Cycle to Cell Fate Decisions. *Trends Cell Biol* 25:592-600.  
383 10.1016/j.tcb.2015.07.007
- 384 Ji Y, Rong X, Li D, Cai L, Rao J, and Lu Y. 2016. Inhibition of Cartilage Acidic Protein 1 Reduces Ultraviolet B  
385 Irradiation Induced-Apoptosis through P38 Mitogen-Activated Protein Kinase and Jun Amino-Terminal  
386 Kinase Pathways. *Cell Physiol Biochem* 39:2275-2286. 10.1159/000447920
- 387 Koshiyama DB, Trevisan P, Graziadio C, Rosa RFM, Cunegatto B, Scholl J, Provenzi VO, de Sa AP, Soares FP,  
388 Velho MC, de APFN, Oliveira CA, and Zen PRG. 2017. Frequency and clinical significance of  
389 chromosome 7 and 10 aneuploidies, amplification of the EGFR gene, deletion of PTEN and TP53 genes,  
390 and 1p/19q deficiency in a sample of adult patients diagnosed with glioblastoma from Southern Brazil. *J*  
391 *Neurooncol* 135:465-472. 10.1007/s11060-017-2606-6
- 392 Kwon MJ, Kang SY, Cho H, Lee JI, Kim ST, and Suh YL. 2019. Clinical relevance of molecular subgrouping of  
393 gliomatosis cerebri per 2016 WHO classification: a clinicopathological study of 89 cases. *Brain Pathol.*  
394 10.1111/bpa.12782
- 395 Langfelder P, and Horvath S. 2008. WGCNA: an R package for weighted correlation network analysis. *BMC*  
396 *Bioinformatics* 9:559. 10.1186/1471-2105-9-559
- 397 Liu B, Liu J, Liu K, Huang H, Li Y, Hu X, Wang K, Cao H, and Cheng Q. 2019. A prognostic signature of five  
398 pseudogenes for predicting lower-grade gliomas. *Biomed Pharmacother* 117:109116.  
399 10.1016/j.biopha.2019.109116
- 400 Maier V, Jolicoeur C, Rayburn H, Takegahara N, Kumanogoh A, Kikutani H, Tessier-Lavigne M, Wurst W, and  
401 Friedel RH. 2011. Semaphorin 4C and 4G are ligands of Plexin-B2 required in cerebellar development.  
402 *Mol Cell Neurosci* 46:419-431. 10.1016/j.mcn.2010.11.005
- 403 Music D, Dahlrot RH, Hermansen SK, Hjelmberg J, de Stricker K, Hansen S, and Kristensen BW. 2016. Expression  
404 and prognostic value of the WEE1 kinase in gliomas. *J Neurooncol* 127:381-389. 10.1007/s11060-015-  
405 2050-4
- 406 Ouyang D, Li R, Li Y, and Zhu X. 2019. A 7-lncRNA signature predict prognosis of Uterine corpus endometrial  
407 carcinoma. *J Cell Biochem* 120:18465-18477. 10.1002/jcb.29164
- 408 Ren Y, Zhang X, Rui W, Pang H, Qiu T, Wang J, Xie Q, Jin T, Zhang H, Chen H, Zhang Y, Lu H, Yao Z, Zhang J,

409 and Feng X. 2019. Noninvasive Prediction of IDH1 Mutation and ATRX Expression Loss in Low-Grade  
410 Gliomas Using Multiparametric MR Radiomic Features. *J Magn Reson Imaging* 49:808-817.  
411 10.1002/jmri.26240

412 Sabha N, Knobbe CB, Maganti M, Al Omar S, Bernstein M, Cairns R, Cako B, von Deimling A, Capper D, Mak  
413 TW, Kiehl TR, Carvalho P, Garrett E, Perry A, Zadeh G, Guha A, and Sidney C. 2014. Analysis of IDH  
414 mutation, 1p/19q deletion, and PTEN loss delineates prognosis in clinical low-grade diffuse gliomas. *Neuro*  
415 *Oncol* 16:914-923. 10.1093/neuonc/not299

416 Sahm F, Koelsche C, Meyer J, Pusch S, Lindenberg K, Mueller W, Herold-Mende C, von Deimling A, and  
417 Hartmann C. 2012. CIC and FUBP1 mutations in oligodendrogliomas, oligoastrocytomas and  
418 astrocytomas. *Acta Neuropathol* 123:853-860. 10.1007/s00401-012-0993-5

419 Shannon P, Markiel A, Ozier O, Baliga NS, Wang JT, Ramage D, Amin N, Schwikowski B, and Ideker T. 2003.  
420 Cytoscape: a software environment for integrated models of biomolecular interaction networks. *Genome*  
421 *Res* 13:2498-2504. 10.1101/gr.1239303

422 Wang X, Zbou C, Qiu G, Fan J, Tang H, and Peng Z. 2008. Screening of new tumor suppressor genes in sporadic  
423 colorectal cancer patients. *Hepatogastroenterology* 55.

424 Wang Z, Wang Z, Niu X, Liu J, Wang Z, Chen L, and Qin B. 2019. Identification of seven-gene signature for  
425 prediction of lung squamous cell carcinoma. *Onco Targets Ther* 12:5979-5988. 10.2147/OTT.S198998

426 Wu M, Li X, Liu Q, Xie Y, Yuan J, and Wanggou S. 2019. miR-526b-3p serves as a prognostic factor and regulates  
427 the proliferation, invasion, and migration of glioma through targeting WEE1. *Cancer Manag Res* 11:3099-  
428 3110. 10.2147/CMAR.S192361

429 Yu G, Wang LG, Han Y, and He QY. 2012. clusterProfiler: an R package for comparing biological themes among  
430 gene clusters. *OMICS* 16:284-287. 10.1089/omi.2011.0118

431 Zeng WJ, Yang YL, Liu ZZ, Wen ZP, Chen YH, Hu XL, Cheng Q, Xiao J, Zhao J, and Chen XP. 2018. Integrative  
432 Analysis of DNA Methylation and Gene Expression Identify a Three-Gene Signature for Predicting  
433 Prognosis in Lower-Grade Gliomas. *Cell Physiol Biochem* 47:428-439. 10.1159/000489954

434 Zhang C, Yu R, Li Z, Song H, Zang D, Deng M, Fan Y, Liu Y, Zhang Y, and Qu X. 2019a. Comprehensive analysis  
435 of genes based on chr1p/19q co-deletion reveals a robust 4-gene prognostic signature for lower grade  
436 glioma. *Cancer Manag Res* 11:4971-4984. 10.2147/CMAR.S199396

437 Zhang GH, Zhong QY, Gou XX, Fan EX, Shuai Y, Wu MN, and Yue GJ. 2019b. Seven genes for the prognostic  
438 prediction in patients with glioma. *Clin Transl Oncol*. 10.1007/s12094-019-02057-3  
439  
440  
441  
442  
443  
444  
445

# Figure 1

Study outline.

The outline indicates the exploration process.

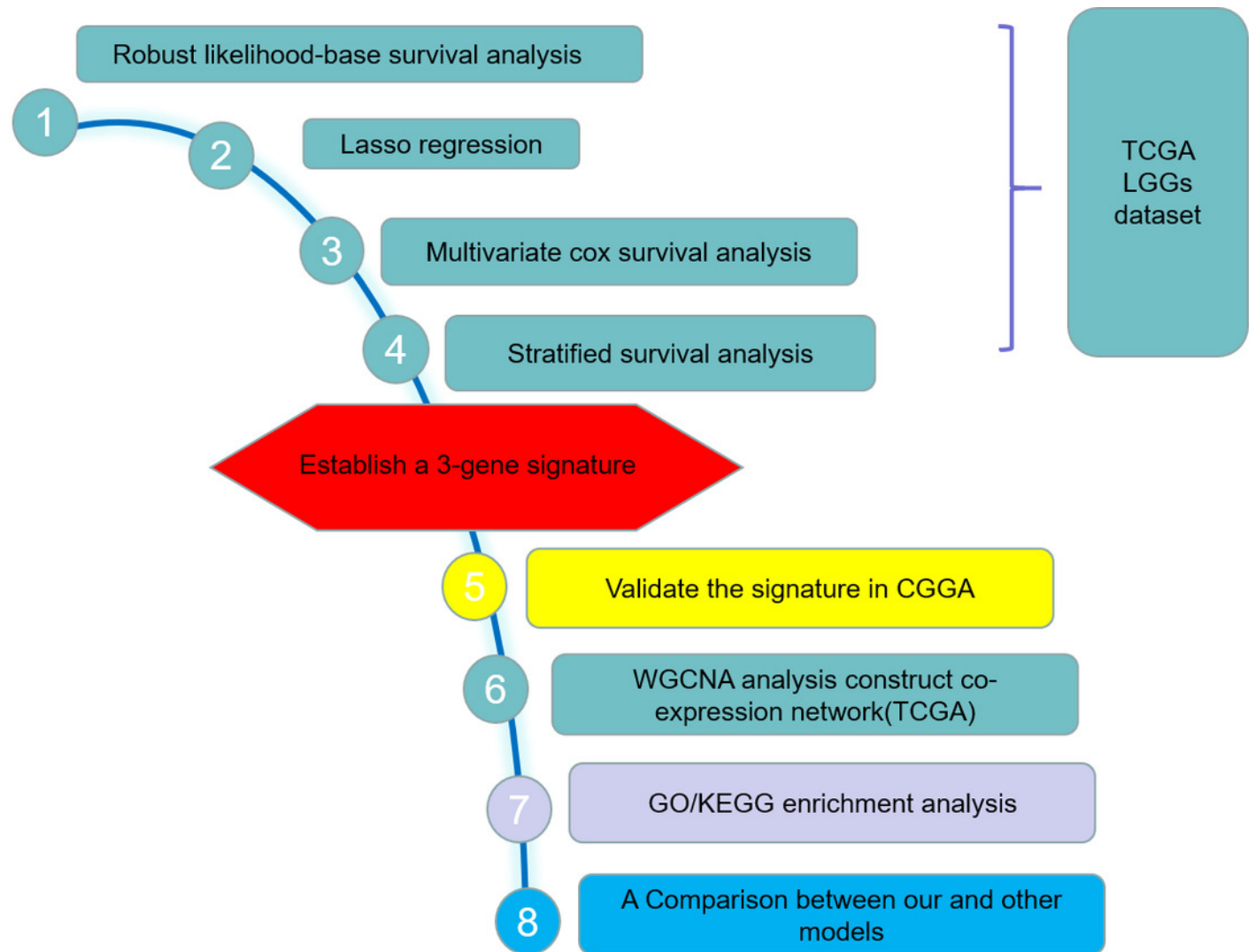


## Figure 2

The LASSO regression used to reduce the dimensionality of survival related genes.

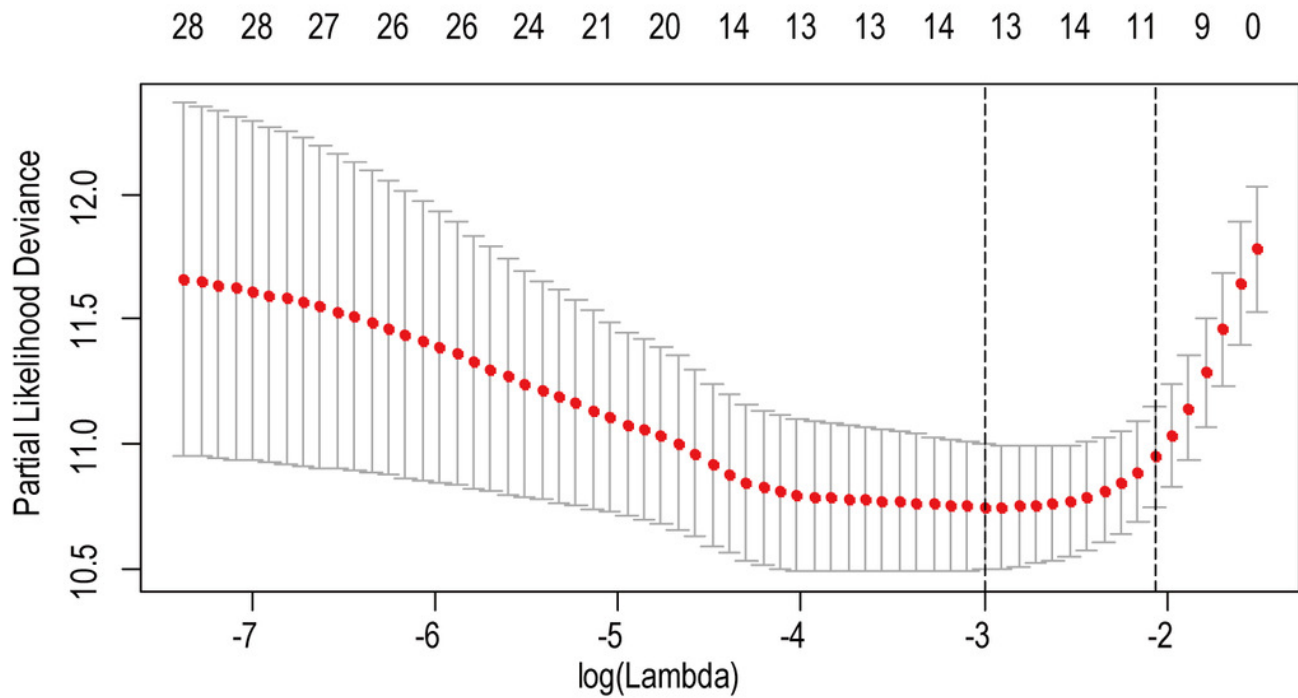


## Figure 3

Risk score analysis, survival status and survival time between two risk group and expression distribution of the three-gene signature in TCGA dataset.

**(A)** The three-gene signature risk score distribution. **(B)** Scatterplot of patient survival status ordered by risk score. **(C)** The heat-map of the three-gene expression profiles after standardized and centralized.

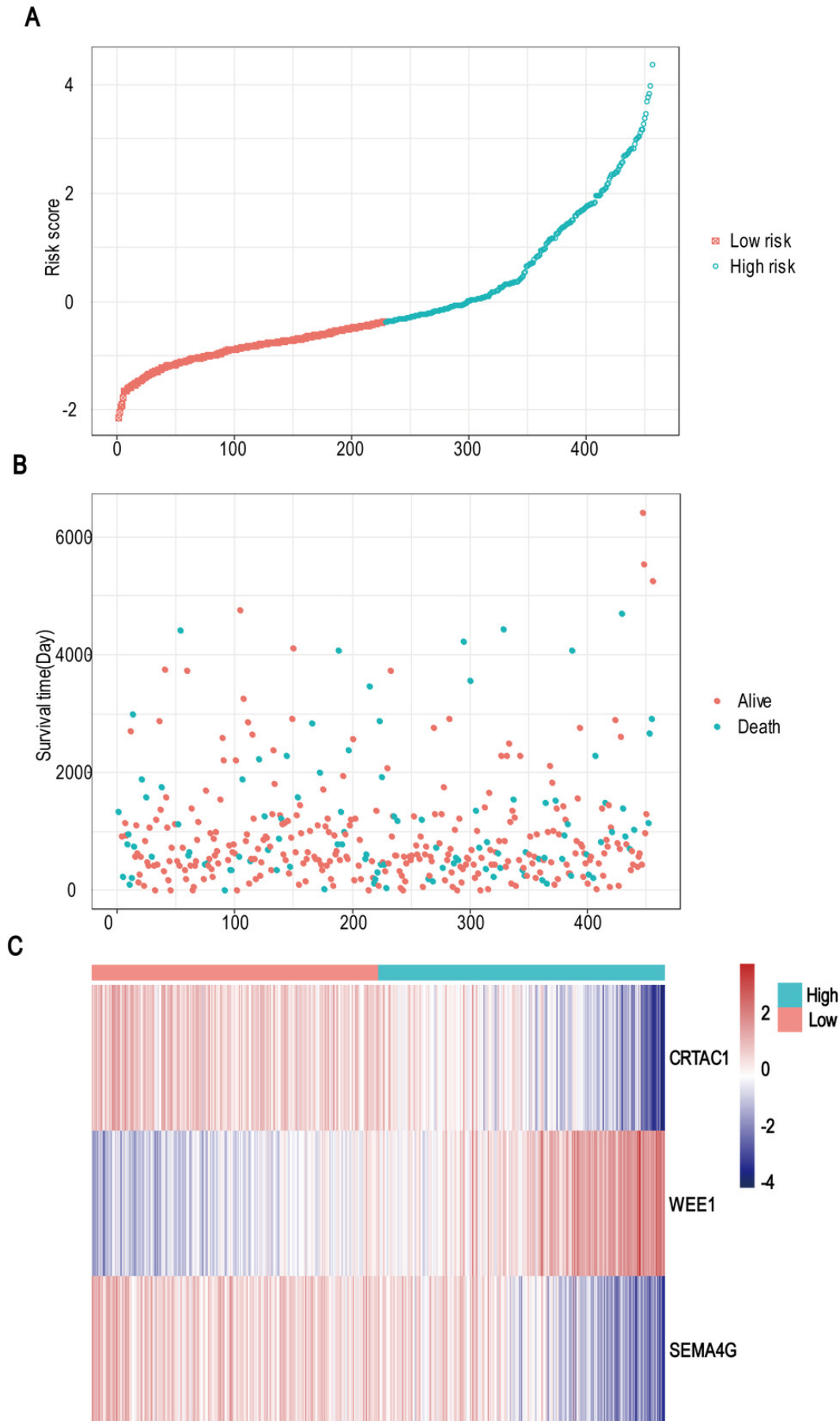


## Figure 4

Establishment and verification of the risk model in the training set and validation set.

**(A)** Patient in high-risk group displayed significantly shorter survival time compared to those in low-risk group in training set ( $P < 0.0001$ ). **(B)** The ROC for predicting the 1-, 3- and 5-year survival and AUC for the risk score model showed good accuracy in training set. **(C, D)** The same result can be observed in the validation set.

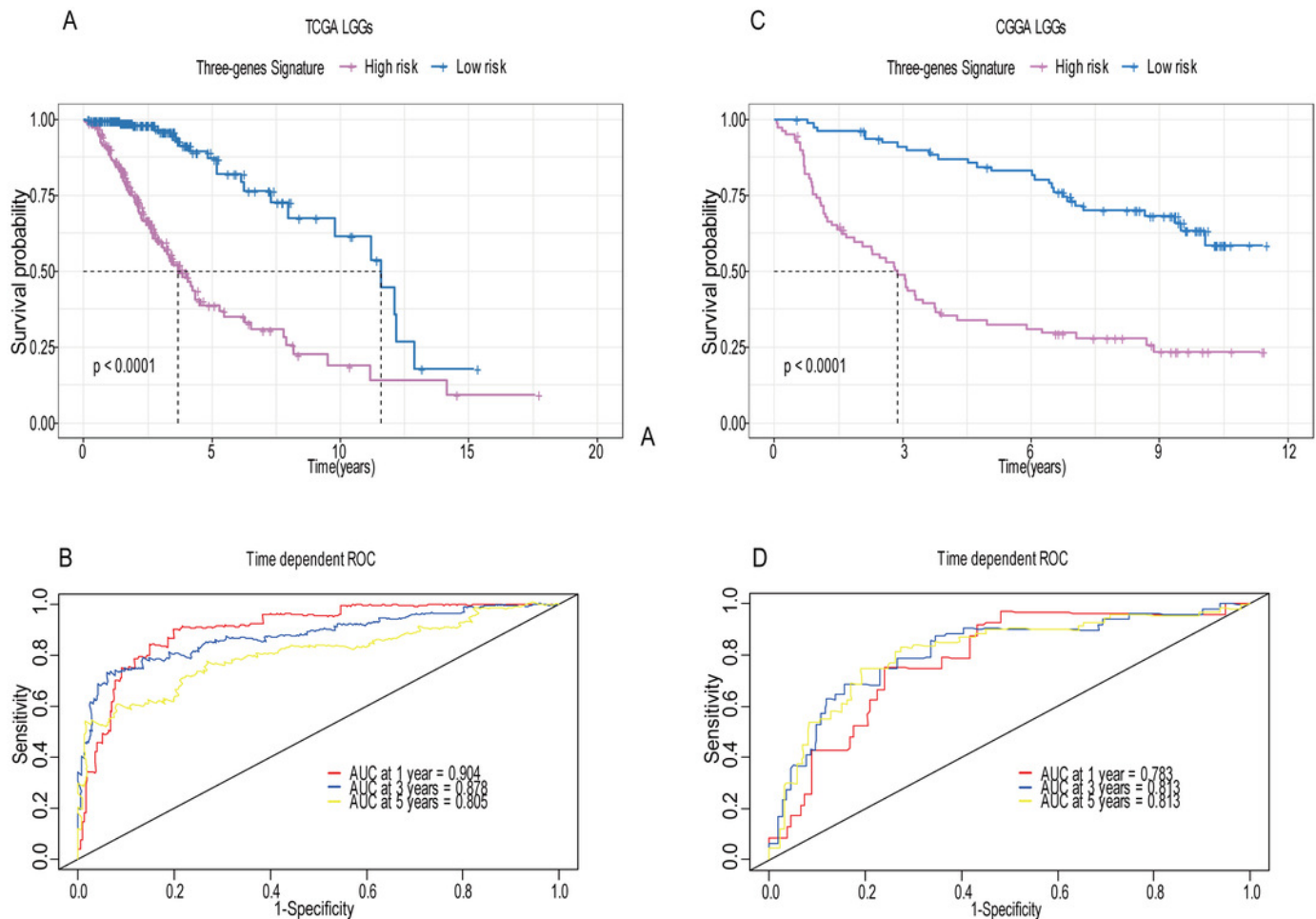


## Figure 5

Stratified survival analysis based on the risk model in the training set.

Based on the risk score model, stratified survival analysis performed in patients with different age group(A-D) gender(B-E) and pathologic grade(C-F) in the training set.

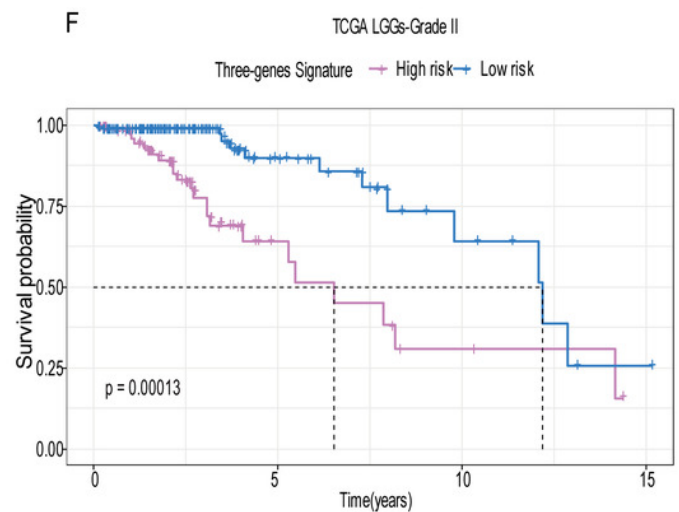
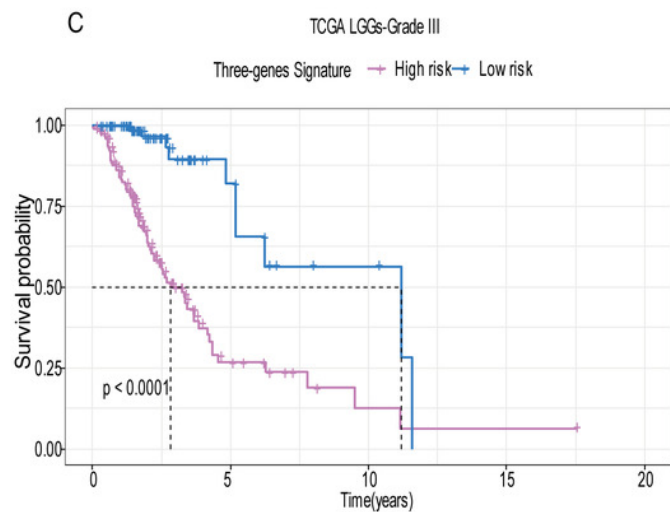
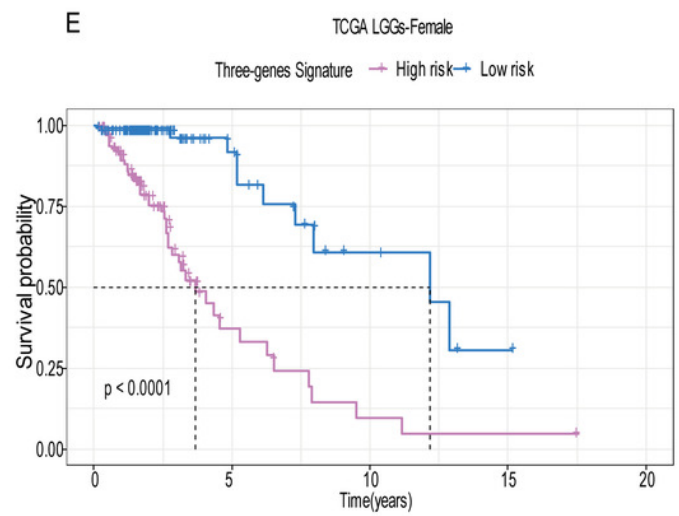
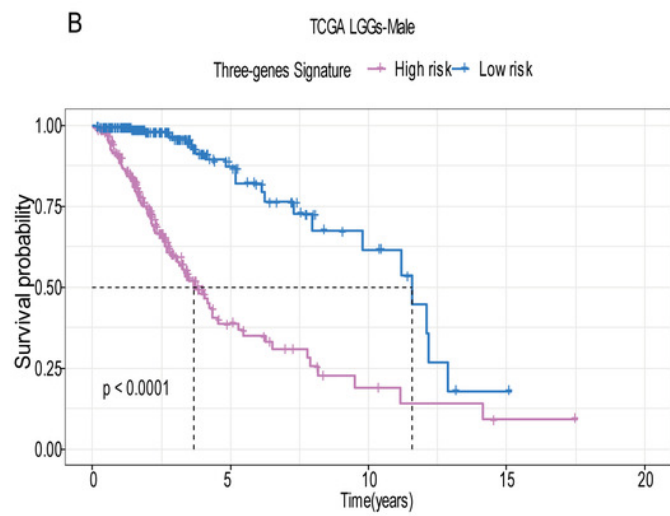
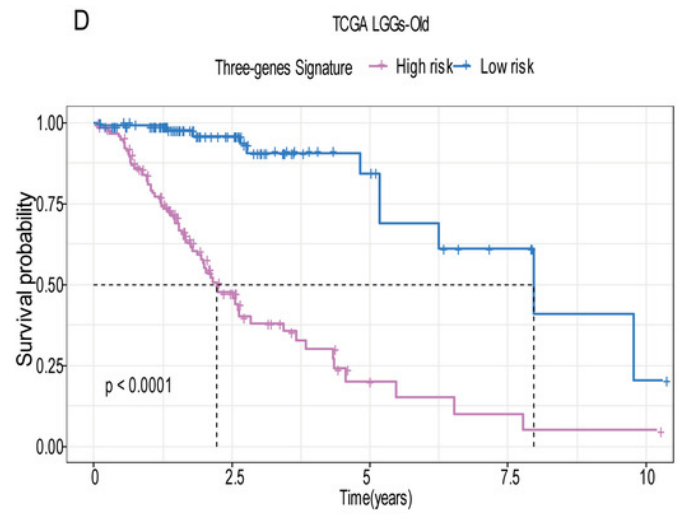
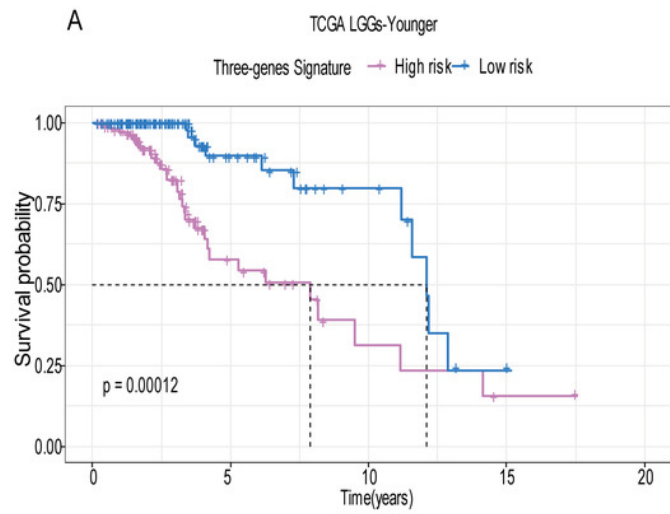


## Figure 6

Stratified survival analysis based on the risk model in the validation set

Based on the risk score model, stratified survival analysis performed in patients with different age group(A-D) gender(B-E) and pathologic grade(C-F) in the validation set.

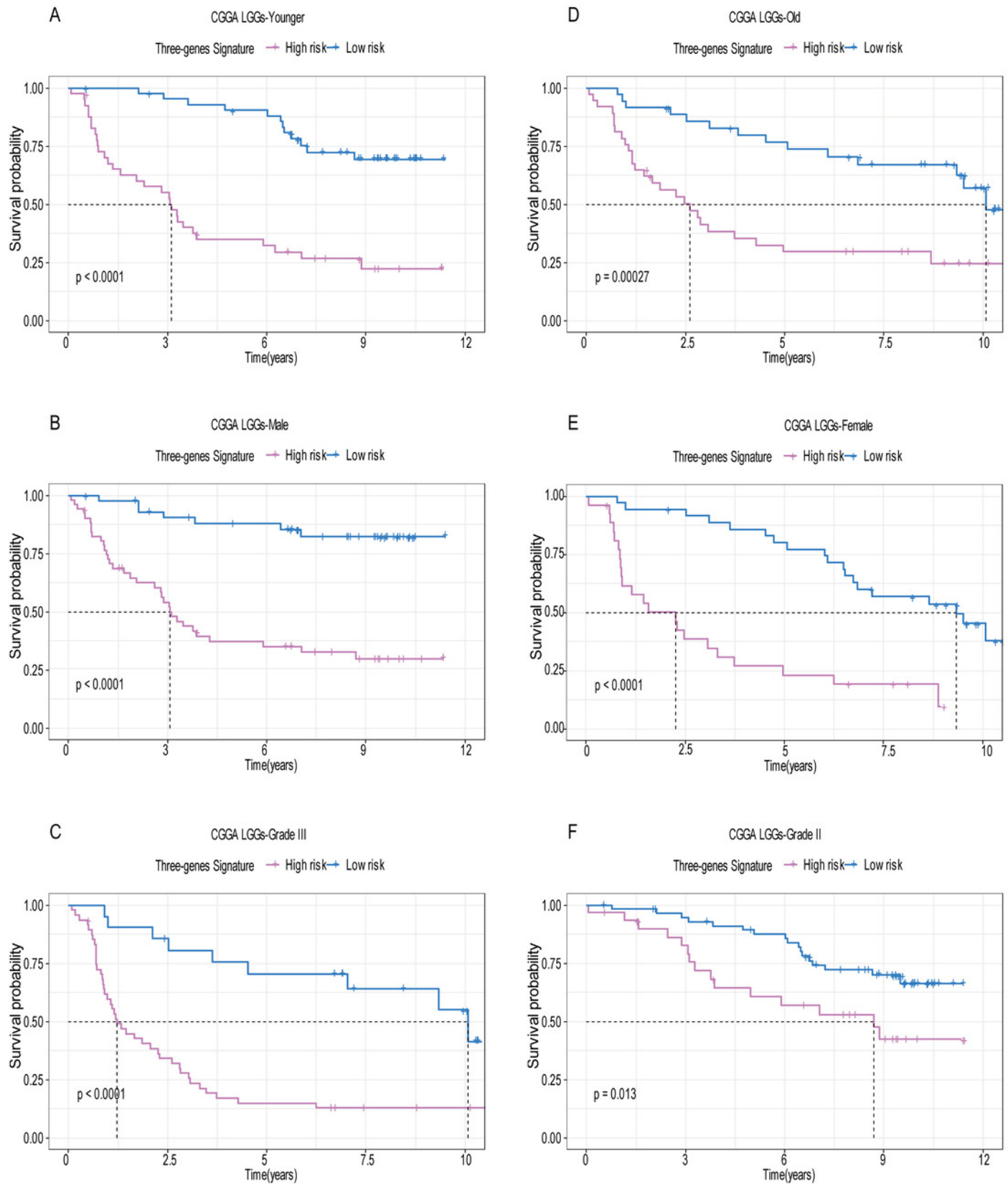


## Figure 7

The expression level of the three genes can divided the patients into different prognostic group in both training set and validation set.

For the WEE1 the member of high expression group had significantly shorter survival than those in low expression group ( $P < 0.0001$ ) (A-D). For the CRTAC1 the member of high expression group had significantly longer survival than those in low expression group ( $P < 0.0001$ ) (B-E). For the SEMA4G the member of high expression group had significantly longer survival than those in low expression group ( $P < 0.0001$ ) (C-F).

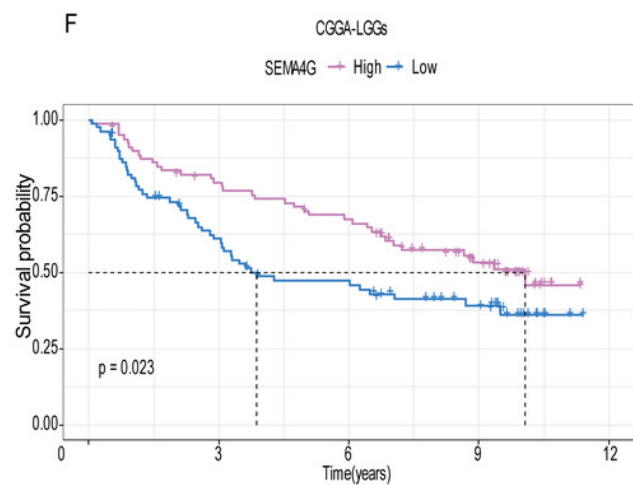
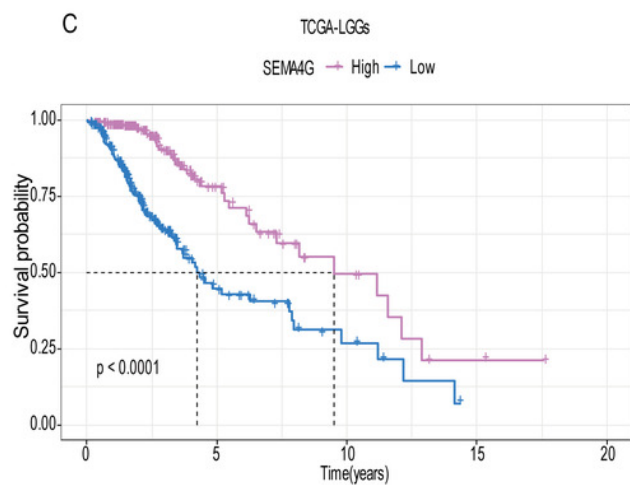
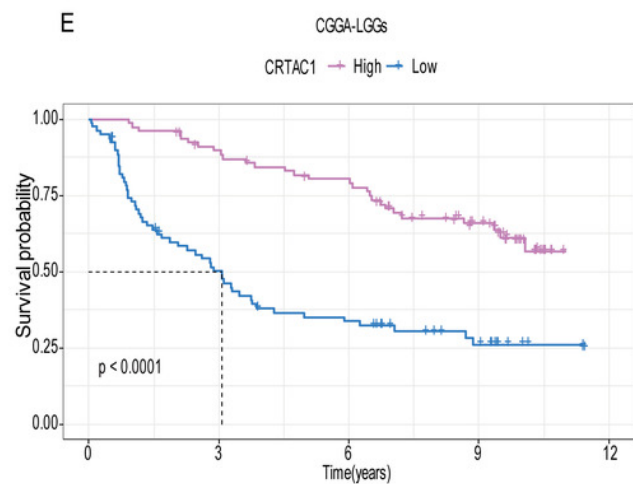
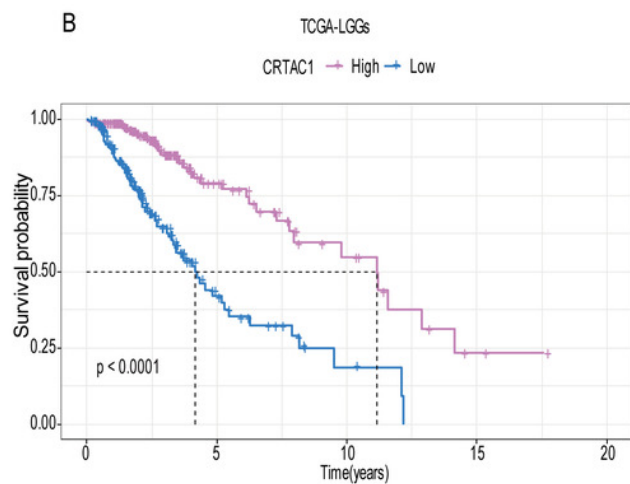
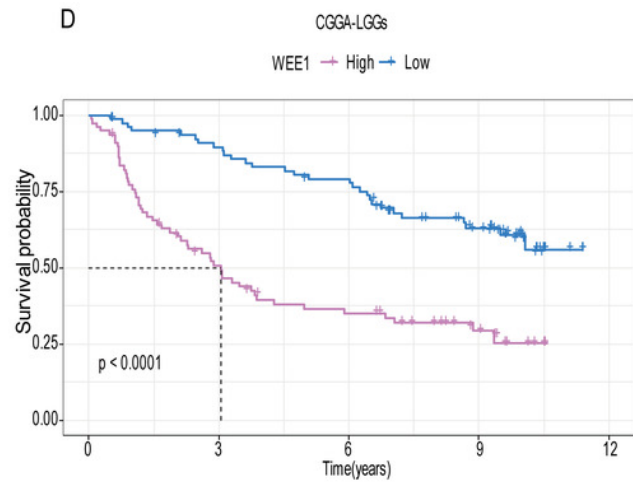
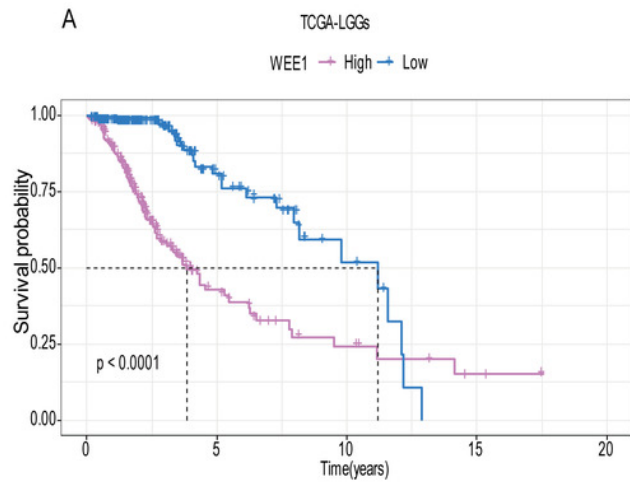


## Figure 8

Expression of the three genes between grade II tumor and grade III tumor in training set and validation set.

In the training set, the expression level of WEE1 was significantly higher in grade III compared to grade II ( $P < 0.0001$ ) while the other are opposite (A). These results can also be verified in the validation dataset (B).

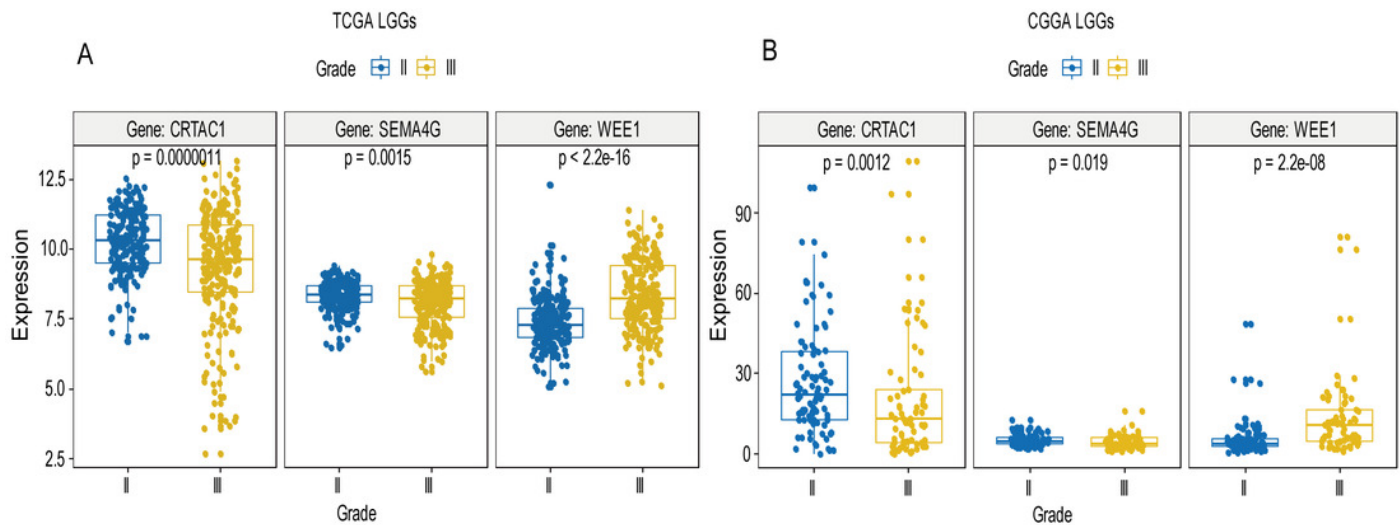
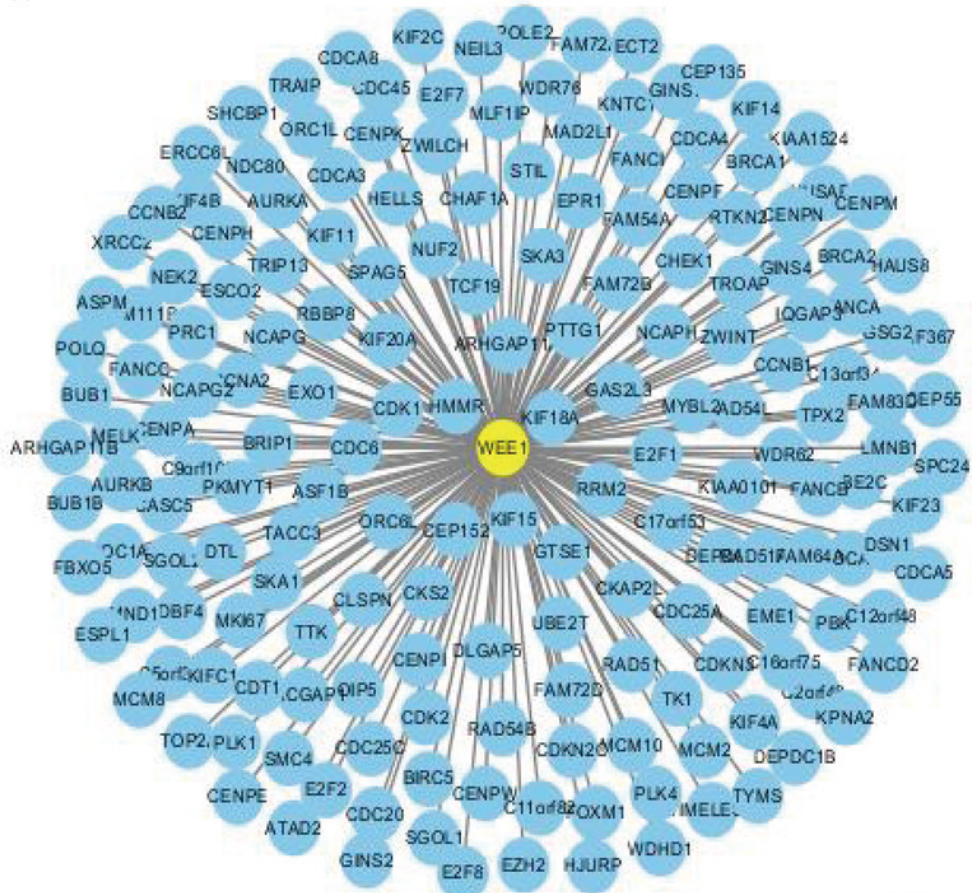


## Figure 9

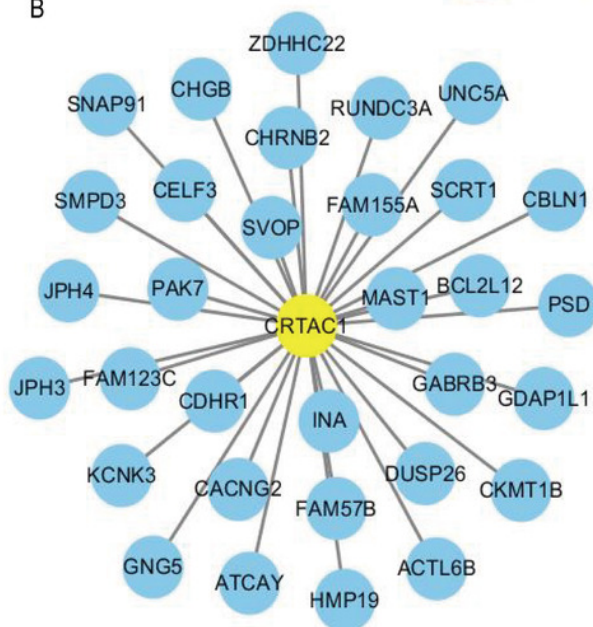
Co-expression network of the three-gene signature.

The co-expression networks of WEE1(A), CRTAC1(B) and SEMA4G(C) were showed. Yellow nodes showed key genes and blue nodes are genes which co-expressed with the key genes.

A



B



C

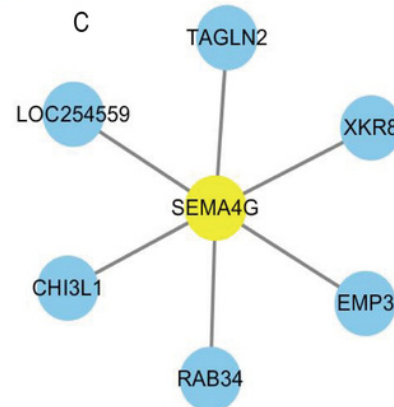


## Figure 10

The most significantly enriched GO annotations and KEGG pathways of co-expressed genes. The length of the bars and the size of the dots represents the numbers of genes, and the color of the bars/dots corresponds to the P-value according to legend.

**(A)** Top 5 significantly enriched biological process. **(B)** Top 5 significantly enriched cellular component. **(C)** Top 5 significantly enriched KEGG pathways. **(D)** Top 5 significantly enriched molecular function.

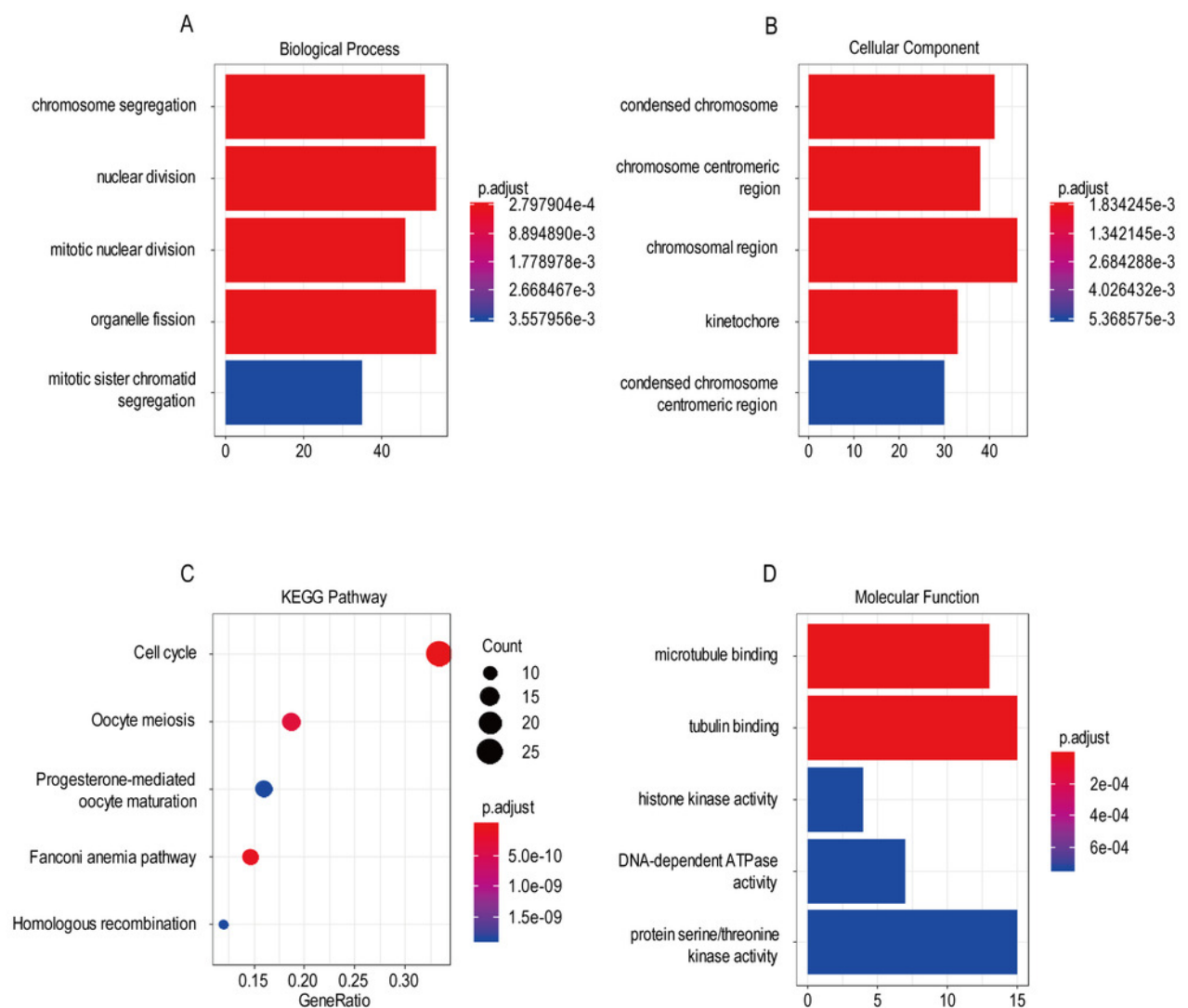


## Figure 11

Comparison of our 3-gene model and other literature models.

The-dependent ROC analysis was performed to compare the three models in predicting 1-year(**A**), 3-year(**B**) and 5-year(**C**) overall survival.

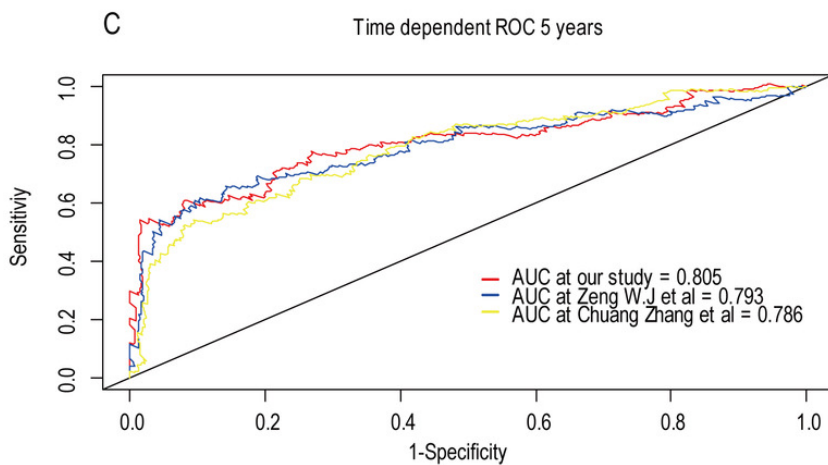
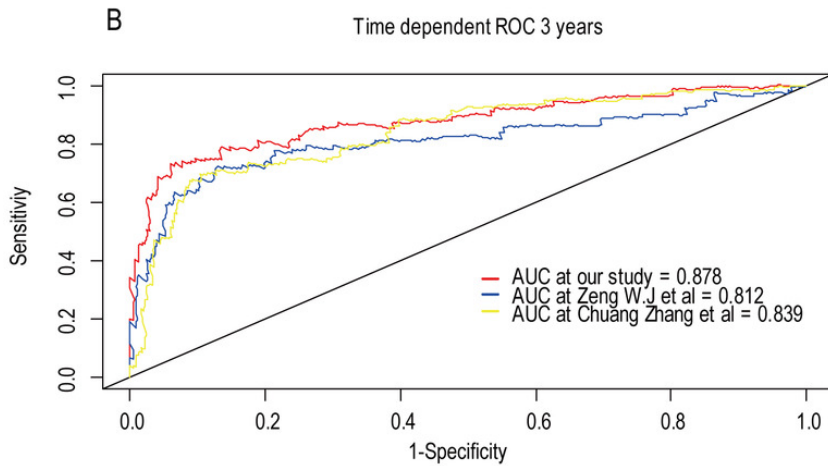
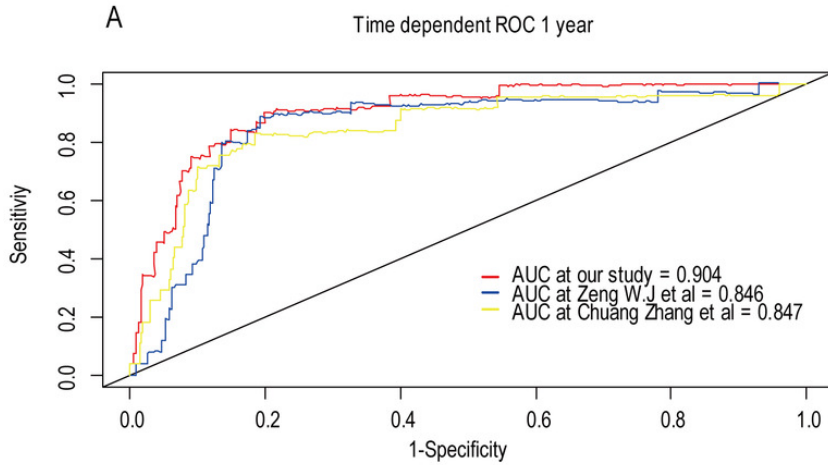


**Table 1** (on next page)

Clinical parameters of patients in the training set and validation set.

1

2 **Table1:**3 **Clinical parameters of patients in the training set and validation set.**

Variables	Training set(n=456)	Validation set(n=159)	Pvalue
Age group(Median)			0.5448
younger	232	86	
old	224	73	
Sex			0.1894
Female	210	63	
Male	246	96	
Grade			0.09385
G2	221	90	
G3	235	69	
Molecular therapy			
Yes	263	/	
NO	193	/	
Chemoterapy			
Yes	/	80	
NO	/	79	
Risk level			1
High	228	79	
Low	228	80	
IDH_status			
Wildtype	/	43	
Mutant	/	116	
1p19q_status			
Non_codel	/	52	
Codel	/	107	
Radiation therapy			3.52E-10
Yes	280	141	
NO	176	18	
Age(years)			
Mean±SD	43.4±13.3	40.7±10.9	0.989
Median	41	40	
Vital status			
Alive	341	77	
Dead	115	82	
Survival time(days)			
Mean	998.6±953.8	2024.7±1334.3	5.27E-

			24
Median	714.5	2340	
Histologic type			
Astrocytoma	162	34	
Oligodendroglioma	171	21	
Oligoastrocytoma	123	35	
Anaplastic astrocytomas	/	26	
Anaplastic oligoastrocytomas	/	32	
Anaplastic oligodendrogliomas	/	11	

---

4

**Table 2** (on next page)

Univariate and multivariate Cox regression analyses of the risk score and other clinicopathological factors in training set and validation set.

Variables		Training set(n=456)						Validation set(n=159)					
		Univariate			Multivariate			Univariate			Multivariate		
		HR	95%CI	p-value	HR	95%CI	p-value	HR	95%CI	p-value	HR	95%CI	p-value
Age group(Median)	younger vs old	0.27	0.184-0.420	<b>1.3E-09</b>	0.27	0.179-0.418	<b>2.21E-09</b>	0.81	0.530-1.261	0.363	1.051	0.654-1.691	0.837
	Sex	1.04	0.721-1.509	0.823	1.08	0.743-1.572	0.686	0.64	0.416-0.989	<b>0.044</b>	0.651	0.412-1.028	0.066
Grade	G3 vs G2	3.30	2.196-4.963	<b>9.3E-09</b>	2.49	1.568-3.953	<b>0.00011</b>	3.59	2.292-5.625	<b>2.4E-08</b>	3.799	2.205-6.545	<b>0.00000151</b>
Molecular therapy	Yes vs No	1.36	0.924-2.018	0.117	0.89	0.578-1.379	0.608	/	/	/	/	/	/
Chemoterapy	Yes vs No	/	/	/	/	/	/	2.21	1.409-3.485	<b>0.00057</b>	1.041	0.614-1.765	0.881
Risk level	Low vs High	0.18	0.118-0.299	<b>2.1E-12</b>	0.19	0.120-0.325	<b>1.68E-10</b>	0.24	0.153-0.394	<b>5.7E-09</b>	0.415	0.251-0.688	<b>0.000653</b>
IDH_status	Wildtype vs Mutant	/	/	/	/	/	/	2.49	1.582-3.937	<b>8.4E-05</b>	0.995	0.600-1.650	0.983
1p19q_status	Non_codel vs Codel	/	/	/	/	/	/	6.55	3.358-12.790	<b>3.6E-08</b>	4.566	2.215-9.414	<b>0.0000388</b>
Radiation therapy	Yes vs No	1.99	1.278-3.118	<b>0.00236</b>	0.81	0.488-1.358	0.43	0.47	0.262-0.861	<b>0.0141</b>	0.524	0.277-0.990	<b>0.046</b>